Spline adjustment for modelling solar intermittences

Ajuste spline para modelar intermitencias solares

Raúl Alberto López-Meraz [iD] [1*], Luis Hernández-Callejo [iD] [2], Luis Omar Jamed-Boza [iD] [1], Victor Alonso-Gómez [iD] [2]

[1]Unidad de Ingeniería y Ciencias Químicas, Universidad Veracruzana. Circuito Universitario Gonzalo Aguirre Beltrán s/n. C. P. 9100. Xalapa, México.
[2]Escuela Universitaria de Ingenierías Agrarias, Universidad de Valladolid. Campus Universitario Duques de Soria s/n. C. P. 42004. Soria, España.

ABSTRACT: One of the reasons why photovoltaic technology is not massively installed is its variation in production. This variation is due to intermittences in the solar resource. Based on real data from the microgrid of the Renewable Energy Development Center (CEDER, Spain) and another scenario in Xalapa (México), the study determines the solar intermittences produced and grouped monthly. The period of data acquisition, in the first study, was from May 30th, 2012 to March 3rd, 2015 with the help of a Baseline Surface Radiation Network (BSNR) team; in the second, 2014 measurements were obtained from a meteorological station certified by the National Meteorological System (SMN). The analysis is based on the determination of monthly frames of reference for radiation by third-degree spline adjustments with smoothing, using the JUMP statistical application software (JMP © 2009, SAS Institute, version 8.0.2). The results of the analyses have provided important information to understand the unstable appearance of solar radiation and, in turn, will be the basis of a control system to optimize photovoltaic production.

RESUMEN: Una de las razones por la cual la tecnología fotovoltaica no se instala de forma masiva es su variación en la producción. Esta variación es debida a las intermitencias en el recurso solar. A partir de datos realesde la microred del Centro de Desarrollo de Energía Renovable (CEDER) y un segundo escenario en Xalapa (México), el estudio determina las intermitencias solares producidas y agrupadas mensualmente.. El periodo de adquisición de datos, en el primer estudio, fue del 30 de mayo de 2012 al 3 de marzo de 2015 con la ayuda de un equipo Baseline Surface Radiation Network (BSNR); en el segundo se obtuvieron mediciones del año 2014 provenientes de una estación meteorológica certificada por el Sistema Meteorológico Nacional (SMN). El análisis se fundamenta en determinar marcos de referencia mensuales de la radiación mediante ajustes spline de tercer grado con suavización, utilizando el software de aplicación estadística JUMP (JMP©2009, Instituto SAS, versión 8.0.2). Los resultados de los análisis proporcionan información importante para comprender el aspecto inestable de la radiación solar y, a su vez, serán la base de un sistema de control para optimizar la producción fotovoltaica.

1. Introduction

In recent years, the trend of energy markets has led to a revival in the interest of on-site small-scale power generation, preferably renewable, called distributed or decentralized generation (DG) [1, 2]. Some factors contributing to the development of this kind of generation are limitations associated with the building of new transmission lines, satisfying the increasing consumer demand and the concern of climate change [2]. The penetration of DG into microgrids is rapidly growing, achieving a high percentage of installed capacity. However, randomness associated with inputs of this kind of energy, like wind and solar radiation, causes variations in the flow of energy significantly affecting the normal operation of electrical systems [3]. This situation leads to important problems in the security of the microgrids, as well as fluctuations in the frequency of the system and restrictions for the qualification of power lines

[4]. Therefore, intermittency complicates the adoption of solar energy in electric networks, since reliable and predictable generation is required.

There are different ways of dealing with the inconvenience of intermittency, among them the main ones are the distributed energy storage (DES) and the intelligent networks. However, in order to ensure safeness and an efficient operation, a forecast for the behavior of the solar radiation is necessary. Previous research has pointed out that photovoltaic intermittency can be anticipated by using numerical models of the weather forecast and through analysis of satellite imaging [5, 6]. Despite this, in recent research papers, there are no methodologies considering solar intermittently with low levels of uncertainty using historical data from radiation, creating frames of reference for designing a reliable backup system.

The present work proposes a way for the identification and quantification of the concept of solar intermittency using as reference model the cubic spline fitting with smoothing in the micro-grid of the Center for the Development of Renewable Energies (CEDER) belonging to the Center for Environmental and Technological Energy Research (CIEMAT) located in Soria, Spain and in the city of Xalapa, Veracruz, Mexico. This tool has served to respond to different problems, among them is the association of environmental variables with radiation [7], the forecast of the demand for electrical energy [8], analysis of contact surface profiles [9], and simultaneous location and mapping for mobile robots [10]. Thus, in this document, the frequency of number of intermittences is 50, 75 and 90% of their appearances, as well as the radiant power to be covered in the same percentages. The present paper is an extension of the research displayed in the Iberoamerican Congress of Smart Cities (ICSC-CITIES 2018) [11]. We begin, in Section 2 describing the case studies and the characterization of the frame of reference, as well as the definition of intermittency. In Section 3, the most important results of the analysis are presented and, finally, the conclusions and ideas for future work are expressed in point 4.

2. Materials and methods

2.1 Case studies

The information used in CEDER was obtained through a Baseline Surface Radiation Network (BSNR) measuring the solar radiation in situ. The period of collection was from May 30, 2012 to March 3, 2015, in total 442,905 five-minute records. For reasons unrelated to the measurement, the information was adjusted according to the corresponding GMT (zero, Soria 2.4° west). On the other hand, the data for the city of Xalapa comes from the

meteorological station code No. 76,688 of the National Meteorological Service (SMN), located at 19°30′45.27″, latitude north, 96°54′14.44″ west longitude of the meridian of Greenwich, with an altitude of 1,368 meters above sea level (masl), obtained in the year 2014 every ten minutes.

The granularity of the measurements used in the sites has several applications, namely: knowledge of the operation of the plants, the balancing of the networks, management of units in real time and automatic generation control [12–14]. On the other hand, in smart grids, the main advantage is the regulation of storage to support the electricity market, it also smoothes the photovoltaic output and avoids large voltage and frequency oscillations [15]. This is the reason why the decision to maintain the periods delivered by the measurement equipment was taken.

The criterion to define the period of analysis was as follows: if it were done on a daily basis, there would be 28, 30 or 31 different characterizations producing an impractical situation, due to the amount of information, and a conclusion of the monthly behavior would not be obtained. If the samples were half-yearly, the seasons of the year would not be considered. If the period of study were every three months, it would involve the seasons; however, they do not necessarily behave similarly. Therefore, it was decided to carry out the study for monthly periods since, around the days 20-23, there is an official change of season, but its characteristics are not yet reflected; that is to say, there are months of transition (March, June, September and December) where the seasonal particularities are not completely fulfilled. On the other hand, this period corresponds, in general, to that of electric billing.

2.2 Monthly reference for solar radiation

The frame of reference closest to the reality of global radiation was chosen among the following tools:

- Classical statistical regression, avoids the randomness and tends to create a function that minimizes them, finding the tendency of the data set.

- Series of time, tries to follow more the experimental points without minimizing. It tends to average the vertical values between the contiguous horizontals.

- Spline fit with smoothing (smoothing b-spline).

Studies have analyzed the performance of spline functions with typical regression. In [16], the cubic spline provides a better description between the solar radiation and the hours of sun, also, the errors between the measured and estimated values were more uniform compared to the linear regression. In [17], the same technique was tested

in three cities in Malaysia, reaching the same results from [16], finding that global radiation decreases faster in relation to the duration of sunlight due mainly to diurnal climate changes.

On the other hand, the autoregressive moving average (ARMA) model is useful to understand and predict the future value of a specific time series,; however, an important requirement for this model is that the time series must be stationary. Nevertheless, the Augmented Dickey–Fuller (ADF) test found that solar radiation is not. In this way, a stabilization stage is necessary to obtain it [18]. Similar to ARMA, the autoregressive integrated moving average (ARIMA) model focuses its analysis on stationary time series and is based on past values of the variable to be predicted, giving greater importance to the recent past than to the distant past [19]. One drawback to using ARIMA models is the procedure for order selection, being subjective and difficult to apply [20]. Another drawback of these techniques is the fixed assumption of historical data, it is assumed, implicitly, that past situation will be invariable in the future.

For what has been described above, a conservative criterion was sought, that is, to anticipate what has happened and intuited can occur, in order to locate how radiation behaves in present time. The first two options tend to go to extremes. In this way, the numerical method of spline type adjustment with third-degree smoothing was preferred, which is the most useful when a trend in the function wants to be achieved, reflecting frequently consistent randomness. This type of adjustment is non-parametric in the sense that it does not have coefficients of some polynomial function that fully represents the state of the system. However, it turns out to be highly satisfactory when the response of the system tends to be variant and oscillating in which traditional methods, such as least squares, fail. It is worth mentioning that the ideal behavior would be a Gaussian curve without any environmental oscillation.

2.3 Spline fitting

Parametric models usually adopt patterns of the normal distribution in its variations inherent in the measurement technique, which means that many events may differ numerically with the fitted model. Non-parametric adjustments are all those that do not obtain a functional relation such as $Y = f(x_1, x_2, ..., x_p)$. Consequently, they do not necessarily use statistical techniques. In particular, the spline model fits to the behaviour of the (sometimes oscillating) information, with any trend, whose distribution function is not known or the characterization of the curve is not easy to solve in a conventional way, that is to say, it does not assume, a priori, a functional form

[21]. This setting has the particularity of unite polynomials by segments through nodes, avoiding producing acute changes in the smooth curve of the model allowing the combination of this type of functions.

The spline model plays an important role in the area of engineering essentially due to its favorable properties in oscillating interpolation, its structure of segmented polynomials and their low complexity of implementation [22]. In this sense, cubic polynomials are the most used because they present an excellent fit to the nodes to admit the change of curvature, optimizing the variation of the adjustment model and its improvement is based on the number of observations considered [23]. According to [24], the decisive reason for its use is the continuity (calculating a polynomial between each pair of consecutive points), ensuring that the first and second derivative of each polynomial at each node are equal. That is, the splined adjustment does not behave as a single polynomial, achieving a unique smoothed curve. The adjustment type spline with smoothing technique corresponds to the area of numerical methods in conjunction with the calculus of variations. To achieve the characteristics mentioned, the function, the first and the second derivative valued at each x-coordinate, should be the same. If we have the set of points (x_i, y_i), the original observed information with $i = 1, 2, ..., n.$, where each x_i can easily be extended to the case of confluent abscissa, meaning that each "x" may contain more than one "y" with some degree of dependency between the adjacent "$x´s$", obtaining a cubic polynomial between each pair of consecutive points is defined with a local variable $t_i = x - x_i$ and their corresponding domain $h_i = x_{i+1} - x_i$ generating $(n-1)$ polynomials whose function, first and second derived are shown in Equations 1 - 3:

$$f = a + bt + ct^2 + dt^3 \qquad (1)$$

$$f' = b + 2ct + 3dt^2 \qquad (2)$$

$$f'' = 2c + 6dt \qquad (3)$$

To solve the function f in (1) and get their four coefficients, conditions of continuity are required in $t = 0$ and $t = h$, where the function f must coincide, the first derivate f' and the second derivate f'' at the ends of each polynomial.

The parameter of smoothing lambda (λ) comes from the formulation of the equations of Euler-Lagrange. When λ tends to zero, the resulting curve (presents "greater acuity" vertical) is the classic cubic C-Spline interpolation [25, 26]. When tends to infinity, the resulting curve tends to the line obtained by least squares adjustment. The Euler-Lagrange equations require a joint minimization of

the Equation 4:

$$\int_{t_{x_1}}^{t_{x_n}} g''(t)^2 dt + p \left\{ \sum_{i=1}^{n} \left(\frac{g\left(t_{x_i}\right) - y_i}{\delta_{y_i}} \right)^2 + z^2 - S \right\} \tag{4}$$

In the above expression, t_{x_i} is the local variable of each polynomials, $g\left(t_{x_i}\right)$ is the joint function of the $(n-1)$ polynomials valued in x_i. The lagrangian parameter p must comply with the expression $pz = 0$ in the obtained minimization. The δy_i are the values that allow creating weightings in the expression calculation process. The auxiliary variable z allows maintaining congruence in the condition $pz = 0$ that is required comply. The variable S is a function of the smoothing parameter λ so that their behavior is similar. Deeper information about the theoretical spline interpolations family development are in suggested references [27, 28]. The shape and smoothness of a spline relies heavily on this value of smoothing, which is selected from a measure that balances the bias and variance of this class of estimators [29].

2.4 Characterization of the frame of reference

In addition to the considerations listed in Section 2.3, the value λ to be used was decided with the criterion of increasing the value of the coefficient of determination (R^2) while maintaining a smooth line (low acuity). In the case studies λ, it remained constant at 10,000 for consistency conditions. Each x-coordinate is confluent and middle vertical responses are obtained to pondering the closest observed values with greater weight. The monthly spline settings were accomplished with the JMP statistical application software [30]. When making the decision to characterize the radiation for monthly periods, five and ten minutes, it is required to obtain a curve that represents each month; this can be parameterized with functions, generally, of third degree or higher with a good R^2 that measures the predictive quality of the model used, its square root represents the correlation coefficient. Thus, 12 characteristic polynomial functions were obtained with high correlations with respect to each setting original spline.

2.5 Intermittence

To use the b-spline function, it was necessary to define the concept of solar intermittency, understood as the decrease in the amount of radiant power, which is function of the geographical position (spatial scale) and the moment in which it is present (scale temporal), received in a place determined by means of a reference pattern.

The difference between the measured radiation and the one found with the splined adjustment indicates the absence or presence of intermittence. If it is negative, it shows its existence in that reading (x) and its magnitude is the amount of power that must supply a back-up system. Individual intermittencies of 5 and 10 minutes or contiguous of longer duration are expected, the adjacent intermittences and their power deficit being accumulated.

3. Results

3.1 Monthly solar radiation in CEDER

The behavior of the global horizontal radiation in the monthly scenarios in CEDER are presented in Figures 1 and 2, the points measured with the splined adjustment obtained are observed.

It is remarkable the presence of two types of days in each month, except in July and August where this difference disappears. The beginning and end of the radiation vary depending on the month, in this regard, as it is might be expected, it is notable that numbers from reading in the summer months lengthen and shorten in the cold months. The spline radiation peaks reach approximately 800 W/m^2 in July and August and 350 W/m^2 in November and January. The correlation coefficients oscillate between 0.664 to 0.893 where the minors correspond to the months of November and March, representing that in spring and autumn there is greater dispersion in information and in summer this is lower.

3.2 Frame of reference characterization in CEDER

Table 1 shows the upward trend of radiation from January to August, due to the climatic stability of the site. In addition, factors such as the amount of information and granularity in the measurement, favor a better approach to reality. According to the scheme presented in the methodology, Table 1 shows the coefficients of the correlations for CEDER. The correlation model is presented in Equation 5:

$$Y_s = \beta_0 + \beta_1 X + \beta_2 X^2 + \beta_3 X^3 + \beta_4 X^4 + \beta_5 X^5 \tag{5}$$

The Table 1 shows that the best values of $R^2{}_{spline}$ are presented in the summer months. On the other hand, the polynomials are adjusted with high values of determination, i.e., the worst month (March) has an $R^2{}_{poly}$ of 0.997 indicating that very high adjustments were achieved. The orders of the monthly polynomials are of 4º and 5º, respectively, the annual analysis presented its best approach with a 6th order function, where the maximum daily value does not exceed 600 W/m^2 on average.
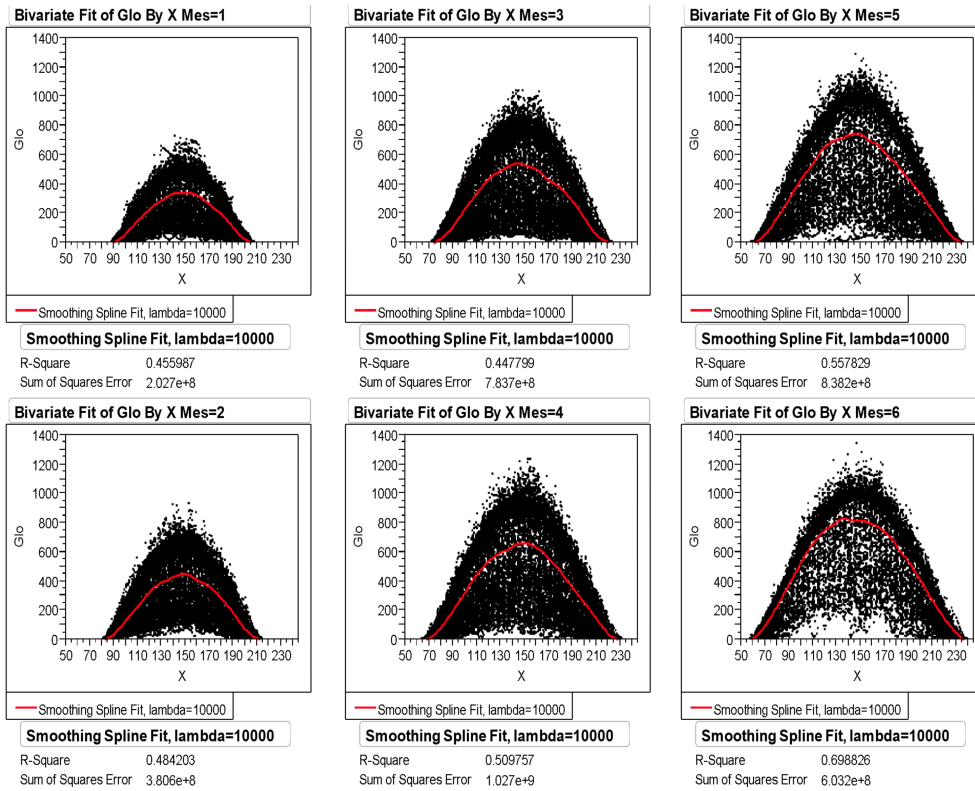
Figure 1 Points observed with the monthly spline adjustments in CEDER in the first half of the year
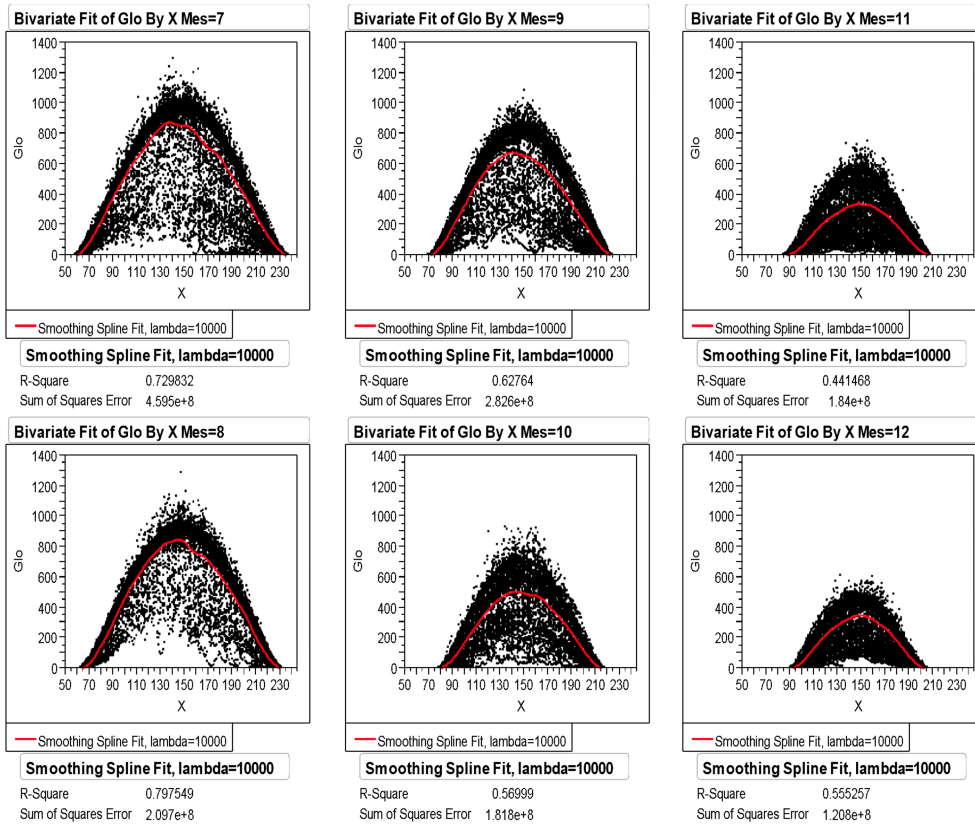

Figure 2 Points observed with the monthly spline adjustments in CEDER in the second half of the year

Table 1 Polynomial coefficients of the spline settings for CEDER

Y(s)	β_0	β_1	β_2	β_3	β_4	β_5	β_6	R^2_{spline}	R^2_{poly}
January	5363.40	-184.14	2.19	-0.011	$1.80e^{-5}$	0	0	0.456	0.999
February	3995.66	-147.08	1.84	$-9.09e^{-3}$	$1.54e^{-5}$	0	0	0.484	0.999
March	1824.19	-83.11	1.18	$-6.17e^{-3}$	$1.06e^{-5}$	0	0	0.448	0.997
April	2005.66	-89.01	1.27	$-6.63e^{-3}$	$1.14e^{-5}$	0	0	0.509	0.999
May	3093.70	-143.05	2.29	-0.015	$4.51e^{-5}$	$-4.96e^{-8}$	0	0.558	0.999
June	482.64	-40.20	0.77	$-4.37e^{-3}$	$7.65e^{-6}$	0	0	0.699	0.998
July	2593.38	-126.41	2.08	-0.014	$3.93e^{-5}$	$-4.10e^{-8}$	0	0.729	0.998
August	3665.83	-168.44	2.66	-0.017	$5.12e^{-5}$	$-5.56e^{-8}$	0	0.797	0.999
September	5436.14	-232.68	3.53	-0.023	$6.99e^{-5}$	$-7.90e^{-8}$	0	0.628	0.999
October	6225.44	-240.55	3.33	-0.020	$5.58e^{-5}$	$-5.64e^{-8}$	0	0.570	0.999
November	5198.98	-177.68	2.11	-0.010	$1.72e^{-5}$	0	0	0.441	0.999
December	6664.63	-224.12	2.63	-0.013	$2.14e^{-5}$	0	0	0.555	0.999
Year	-6260.11	339.97	-7.43	0.083	$-4.82e^{-4}$	$1.40e^{-6}$	$-1.61e^{-9}$	0.339	0.998

Table 2 Quantification of intermittencies and their power in CEDER

Y(s)	N	$I \leq 50$	$I \leq 75$	$I \leq 90$	$P \leq 50$	$P \leq 75$	$P \leq 90$
January	608	3	10	27	98.3434	565.6	2,298.29
February	922	3	8	22	135.005	518.771	2,594.29
March	1,029	3	8	20	174.54	700.096	2,999.96
April	1,240	3	8	21	253.786	1,027.24	3,546.14
May	1,099	2	6	17	231.496	740.902	2,732.03
June	1,159	2	5	12	221.247	788.056	2,333.1
July	802	2	5	14	175.032	692.386	2,066.56
August	579	3	6	16	222.85	685.05	1,936.69
September	555	2	6	17	234.526	747.619	2,542.57
October	518	3	7	16	155.279	600.493	2,110.45
November	664	3	9	27	111.992	461.274	1,861.72
December	548	3	8	25	68.6829	385.447	1,939.83

3.3 Intermittencies in CEDER

According to the previous relationships, the accounting of the intermittences and their powers are presented in Table 2. The lesser-equal intermittences (I) to 50, 75 and 90% are appreciated as well as the deficits of their powers (P). Table 2 shows that in all the months there were, at 50%, maximum of three intermittencies with a period of 15 minutes, December would need less supply because its deficit is 68.6829 W/m². On the other hand, the maximum duration at 75% of the intermittences was 50 minutes, although the monthly average does not exceed 40 minutes. At 90%, the interval ranges from one hour to two hours with 15 minutes. It is notable that the cold months are the ones that present the highest number of intermittences in the three categories; however, their deficits at 50% are the lowest with an average lower than 100 W/m². Obviously, it is observed that the month with the greatest power insufficiency is April. It is noteworthy that there are 5 months (May-September) with very similar conditions in the number of failures and their power deficits. It can be said that the best month is July, both in the number of intermittencies and in their deficits.

3.4 Monthly solar radiation in Xalapa

Figures 3 and 4 show the monthly behavior in Xalapa with its respective spline adjustment.

The maximum radiation was reached in the period from 11:40 to 12:50 hrs, with values from 500 to 825 W/m²; the period of sunlight includes from 6:20 to 19:40 hrs. April and August are the months with the highest solar resource and with the best correlation coefficient (r) 0.802 and 0.768, on the contrary, November has an r of 0.626. It is easier to identify the existence of the two types of days than in CEDER.

3.5 A frame of reference characterization in Xalapa

In contrast to the tendency of CEDER, the direction of the radiation is decreasing, reaching its maximum value in April. This behavior is explained by the presence
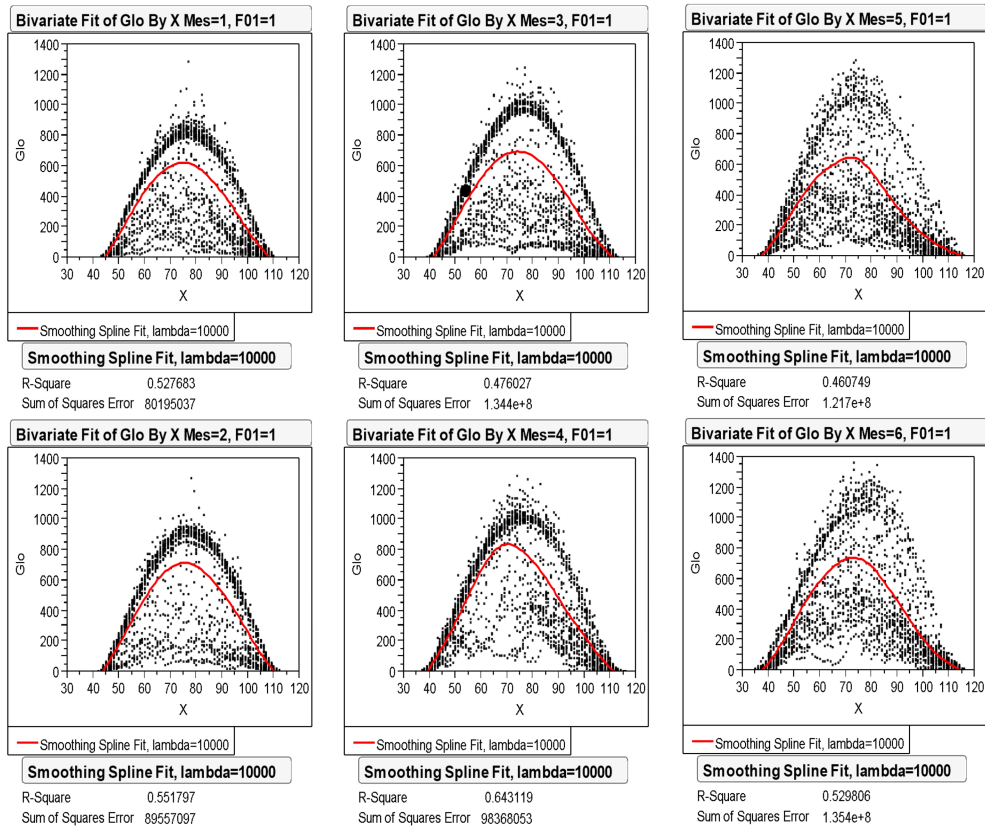
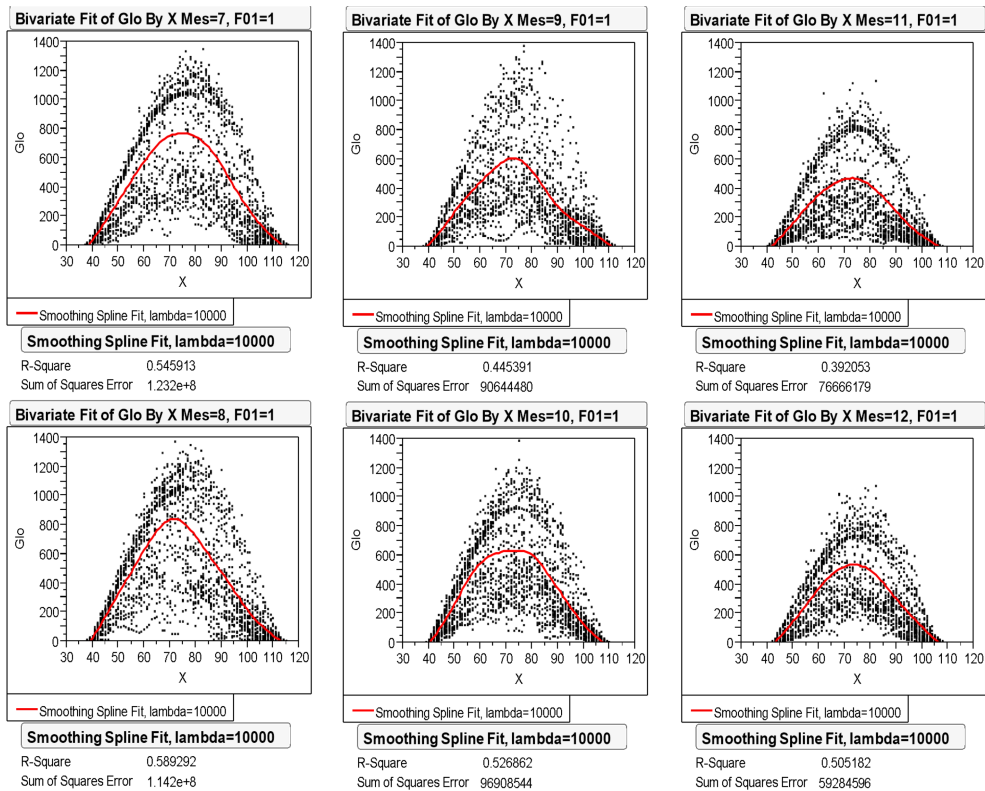**Figure 3** Points observed with the monthly spline adjustments in Xalapa in the first half of the year

Figure 4 Points observed with the monthly spline adjustments in Xalapa in the second half of the year

Table 3 Polynomial coefficients of the spline settings for Xalapa

Y(s)	β_0	β_1	β_2	β_3	β_4	β_5	R^2_{spline}	R^2_{poly}
January	4,236.62	-337.02	8.73	-0.087	$2.96e^{-4}$	0	0.528	0.999
February	4,783.42	-368.30	9.35	-0.092	$3.05e^{-4}$	0	0.552	0.999
March	3,638.01	-299.32	7.99	-0.081	$2.76e^{-4}$	0	0.476	0.999
April	19,428.83	-1,490.87	42.60	-0.562	$3.50e^{-3}$	$-8.33e^{-6}$	0.643	0.999
May	10,050.49	-801.49	23.42	-0.309	$1.89e^{-3}$	$-4.33e^{-6}$	0.461	0.996
June	3,619.66	-298.91	8.14	-0.084	$2.93e^{-4}$	0	0.530	0.998
July	4,939,26	-371.74	9.49	-0.094	$3.18e^{-4}$	0	0.546	0.999
August	17,809.17	-1,347.54	37.86	-0.489	$2.95e^{-3}$	$-6.78e^{-6}$	0.590	0.996
September	16,123.03	-1,210.47	33.97	-0.442	$2.70e^{-3}$	$-6.28e^{-6}$	0.445	0.989
October	2,935.60	-266.47	7.58	-0.081	$2.88e^{-4}$	0	0.527	0.998
November	4,994.14	-366.64	9.26	-0.093	$3.26e^{-4}$	0	0.392	0.999
December	6,830.64	-480.21	11.70	-0.115	$3.94e^{-4}$	0	0.505	0.998
Year	4,804.54	-366.89	9.47	-0.096	$3.29e^{-4}$	0	0.474	0.997

Table 4 Quantification of intermittencies and their power in Xalapa

Y(s)	N	$I \leq 50$	$I \leq 75$	$I \leq 90$	$P \leq 50$	$P \leq 75$	$P \leq 90$
January	114	2	8	22	268.166	835.058	3,187.31
February	92	2	6	12	215.653	679.981	2,897.18
March	125	3	9	21	285.348	1,489.660	5,081.15
April	185	2	6	14	236.719	702.054	2,158.86
May	201	3	5	15	234.274	631.114	1,818.46
June	252	2	5	11	247.169	599.410	1,460.88
July	230	2	4	10	270.574	536.810	1,596.52
August	246	2	4	11	251.400	605.232	1,637.54
September	213	2	6	13	195.276	801.367	1,817.40
October	215	2	6	15	268.940	703.220	1,828.00
November	117	3	12	31	166.043	1,098.720	4,823.10
December	174	3	6	17	220.733	846.074	2,140.10

of continuous cloudiness throughout the year, causing greater variability in the radiation. Other causes in the remoteness of high values R^2 are the number of data and the interval of its acquisition. However, in both places, the month with the lowest solar potential is November, reflecting the worst R^2. Possibly the biggest difference is found in the annual polynomial adjustment, in the case CEDER a 6th function was necessary and in Xalapa it was 4th.

Table 3 shows the coefficients of the correlations for Xalapa. The table presents the same situation in the orders of the polynomial models even with the smallest number of records, at the same time, the same R^2_{poly} is reached in both cases. The polynomial regressions of the spline adjustments were elaborated at 5% significance $(\alpha = 0.05)$, all β coefficients being significant.

3.6 Intermittencies in Xalapa

The accounting of the intermittences and their powers are presented in Table 4. The lesser-equal intermittences (I)

to 50, 75 and 90% are appreciated as well as the deficits of their powers (P).

As shown in Table 4, all months showed a maximum of three intermittencies at 50%, with a maximum period of 30 minutes. On the other hand, the maximum duration at 75% of all the intermittences was 120 minutes, although the monthly average does not exceed 70 minutes. Five hours 10 minutes was the maximum time with 90% of the intermittences. The maximum cumulative intermittencies are presented in November, January and March and the lowest in summer (June-August). As in CEDER, the best month is July, although the lack of power at 50% of the intermittences is the second most important in magnitude. In the months of seasonal transition, March and the second half of autumn (November and December), the greatest number of intermittences was obtained, as expected in these stations. However, November would need less supply since its power deficit level at 50% is the lowest with 166.043 W/m^2; in contrast, March is the month that requires the most support. The most favorable months of the solar resource are from June to August

where the number of intermittences is less than 50, 75 and 90% respectively, and, consequently, the power to be back will be close to 34% of the maximum power.

In both cases of study, 50% of the intermittences do not exceed the 3 joint ones, at 75 and 90% the values are similar, although the dispersion is greater in Xalapa. With regard to power deficits, in general, it can be seen that in CEDER less power is lost; however, the average values in the three sections are close. As expected, in Xalapa, due to the measurement, there is a longer duration in the intermittences; however, these amounts are similar to twice the time in CEDER.

The annual analyses were omitted because they do not reflect the monthly or seasonal behaviors, hiding random variations, complicating the calculation of the power to be maintained in each month. On the other hand, [31] mentions that most intermittences produce a decrease in the power of 20-30% and that these remain less than a minute, also ensures that if the intermittences are maintained up to six hours cause losses of 80%. In contrast, studies [5, 6] are not able to predict ten minutes intermittencies, being this period of great interest because of the number of existing events.

4. Conclusions

The inherent variation of solar energy is the main challenge to maintain the quality of energy and the reliability of the photovoltaic generation. Hence, the importance of knowing the magnitude and duration of the intermittences. The proposed methodology helps to quantify the number and power loss of these interruptions, demonstrating that the spline model adjusts faithfully to the unstable behavior of solar radiation. The expressions found serve as a basis for making statistically reliable predictions.

The exposed technique, as it was proved, can be used with the information of any set of meteorological stations, in microscale, local-scale or mesoscale through networks of stations. In addition, the models maintain conservative conditions to obtain a monthly energy reserve, offsetting decreases caused by interruptions and achieving stable support systems with low ranges of uncertainty. In general, for a possible alternative system in Xalapa, it is suggested to design it taking into account the greater deficit to 90%, being this approximately 5 kW and for CEDER of 3.5 kW. The analysis made, leaves out 10% of contiguous intermittences that could be fed by the electrical network. This study will be used to manage solar production with a turbine-pumping system to supply the demand profile of the CEDER. The differences found in the case studies are mainly due to the type of climate present. According to the World Meteorological System (WMS), Soria has a temperate climate between the characteristics of Mediterranean and Oceanic with an approximate altitude of 1,100 masl. On the other hand, Xalapa belongs to a temperate high mountain climate, mainly near the Cofre de Perote mountain ($\approx$ 4,200 masl).

5. Acknowledgements

References

[1] M. Abdollahi and G. B. Gharehpetian, "Dynamic performance enhancement of microgrids by advanced sliding mode controller," *Electrical Power and Energy Systems*, vol. 33, no. 1, January 2011. [Online]. Available: https://doi.org/10.1016/j.ijepes.2010.08.011

[2] J. M. Guerrero and *et al.*, "Distributed generation: Toward a new energy paradigm," *IEEE Industrial Electronics Magazine*, vol. 4, no. 1, March 2010. [Online]. Available: https://doi.org/10.1109/MIE.2010.935862

[3] B. V. Mathiesen, H. Lund, and K. Karlsson, "100% renewable energy systems, climate mitigation and economic growth," *Applied Energy*, vol. 88, no. 2, February 2011. [Online]. Available: https://doi.org/10.1016/j.apenergy.2010.03.001

[4] S. Chowdhury, S. P. Chowdhury, and P. Crossley, *Microgrids and Active Distribution Networks*, 1st ed. London, UK: The Institution of Engineering and Technology, 2009.

[5] E. Lorenz, D. Heinemann, H. Wickramarathne, H. G. Beyer, and S. Bofinger. (2007) Forecast of ensemble power production by grid-connected pv systems. [Online]. Available: https://bit.ly/2Xzu0bM

[6] R. Perez and *et al.*, "Validation of short and medium term operational solar radiation forecasts in the US," *Solar Energy*, vol. 84, no. 12, December 2010. [Online]. Available: https://doi.org/10.1016/j.solener.2010.08.014

[7] R. A. López, L. Hernández, J. A. D. Ángel, and Q. Hernández, "Relationship between environmental variables and the performance of solar radiation using the spline fit," *Dyna Energía y Sostenibilidad*, vol. 5, January 2016. [Online]. Available: http://dx.doi.org/10.6036/ES8138

[8] A. F. Barrientos, J. Olaya, and V. M. González, "Un modelo spline para el pronóstico de la demanda de energía eléctrica," *Revista Colombiana de Estadística*, vol. 30, no. 2, pp. 187–202, Dec. 2007.

[9] J. Bedolla and *et al.*, "Aproximación de perfiles discretos en elementos de contacto de ensambles mecánicos," *Ing. invest. y tecnol.*, vol. 14, no. 1, pp. 99–111, Jan. 2013.

[10] A. Toriz and A. Sánchez, "Exploración integrada probabilista para robots móviles en ambientes complejos," *Computación y Sistemas*, vol. 18, no. 1, January 2014. [Online]. Available: http://dx.doi.org/10.13053/CyS-18-1-2014-028

[11] R. A. Lopez, L. Hernández, L. O. Jamed, and V. A. Gomez, "Solar intermittency with spline fit modeling. microgrid case CEDER, soria, spain," in *I Ibero-American Congress of Smart Cities (ICSC-CITIES 2018)*, Soria Spain, 2018, pp. 592–601.

[12] R. H. Inman, H. T. C. Pedro, and C. F. M. Coimbra, "Solar forecasting methods for renewable energy integration," *Progress in Energy and Combustion Science*, vol. 39, no. 6, December 2013. [Online]. Available: https://doi.org/10.1016/j.pecs.2013.06.002

[13] E. Wiemken, H. G. Beyer, W. Heydenreich, and K. Kiefer, "Power characteristics of pv ensembles: experiences from the combined power production of 100 grid connected pv systems distributed over the area of germany," *Solar Energy*, vol. 70, no. 6, 2001. [Online]. Available: https://doi.org/10.1016/S0038-092X(00)00146-8

[14] K. Otani, J. Minowa, and K. Kurokawa, "Study on areal solar irradiance for analyzing areally-totalized pv systems," *Solar Energy Materials and Solar Cells*, vol. 47, no. 1-4, October 1997. [Online]. Available: https://doi.org/10.1016/S0927-0248(97)00050-0

[15] C. Wan, "Photovoltaic and solar power forecasting for smart grid energy management," *CSEE Journal of Power and Energy Systems*, vol. 1, no. 14, December 2015. [Online]. Available: https://doi.org/10.17775/CSEEJPES.2015.00046

[16] A. Genç and *et al.*, "Statistical analysis of solar radiation data using cubic spline functions," *Energy Sources*, vol. 24, no. 12, November 10 2002. [Online]. Available: https://doi.org/10.1080/00908310290087058

[17] R. E. Childs, D. G. S. Chuah, S. L. Lee, and K. C. Tan, "Analysis of solar radiation data using cubic splines," *Solar Energy*, vol. 32, no. 5, 1984. [Online]. Available: https://doi.org/10.1016/0038-092X(84)90141-5

[18] H. Diagne, P. Lauret, M. David, and J. W. Boland, "Solar irradiation forecasting: state-of-the-art and proposition for future developments for small-scale insular grids," *World Renewable Energy Forum*, May 2012.

[19] A. Pankratz, *Forecasting with Univariate Box-Jenkins Models: Concepts and Cases*. United States: John Wiley & Sons, 1983.

[20] R. Hyndman and *et al.*, *forecast: Forecasting functions for time series and linear models*, 2019, R package version 8.7. [Online]. Available: http://pkg.robjhyndman.com/forecast

[21] A. W. Bowman and A. Azzalini, *Applied Smoothing Techniques for Data Analysis: The Kernel Approach with S-Plus Illustrations*, ser. Oxford Statistical Science Series. OUP Oxford, 1997.

[22] D. Petrinovic, "Causal cubic splines: Formulations, interpolation properties and implementations," *IEEE Transactions on Signal Processing*, vol. 56, no. 11, November 2008. [Online]. Available: https://doi.org/10.1109/TSP.2008.929133

[23] S. Couture, J. C. Beal, and Y. M. M. Antar, "The cubic spline interpolation of a standing wave envelope," IEEE Antennas and Propagation Society International Symposium 1992 Digest, Chicago, USA, 1992.

[24] G. Wolberg and I. Alfy, "Monotonic cubic spline interpolation," in *1999 Proceedings Computer Graphics International*, June 1999, pp. 188–195.

[25] J. Mathews and F. Fink, *Numerical Methods Using MATLAB*, 3rd ed. Englewood Cliffs, NJ: Prentice-Hall, Inc., 1999.

[26] M. Grasselli and D. Pelinovsky, *Numerical Mathematics*. Jones & Bartlett Publishers, 2008.

[27] C. Reinsh, "Smoothing by spline functions„" *Numerische Mathematik*, vol. 10, pp. 177–183, 1967.

[28] B. W. Silverman, "Some aspects of the spline smoothing approach to non-parametric regression curve fitting," *Journal of the Royal Statistical Society, Series B (Methodological)*, vol. 47, no. 1, September 1985. [Online]. Available: https://doi.org/10.1111/j.2517-6161.1985.tb01327.x

[29] W. Härdle, *Applied Nonparametric Regression (Econometric Society Monographs)*. Cambridge, UK: Cambridge University Press, 1992.

[30] SAS Institute Inc. (2009) JMP 8.0.2 Release Notes. SAS Institute Inc. DescripciónCary, NC. [Online]. Available: http://www.jmp.com/support/notes/41/addl/fusion_41004_6_releasenotes8_0_2.pdf

[31] V. T. Jayadevan, J. Rodriguez, V. P. A. Lonij, and A. Cronin, "Forecasting solar power intermittency using ground-based cloud imaging," in *World Renewable Energy Forum, WREF 2012, Including World Renewable Energy Congress XII and Colorado Renewable Energy Society (CRES) Annual Conference*, Denver, USA, 2012, pp. 2100–2106.